

Ion-Selective Controlled Assembly of Dendrimer-Based Functional Nanofibers and Their Ionic-Competitive Disassembly

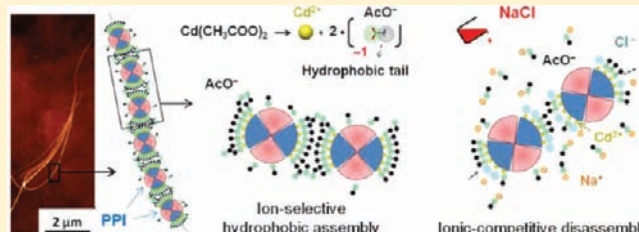
Matteo Garzoni,[†] Nicolas Cheval,^{‡,§} Amir Fahmi,^{*,‡,§} Andrea Danani,[†] and Giovanni M. Pavan^{*,†}

[†]Laboratory of Applied Mathematics and Physics (LaMFI), University of Applied Sciences of Southern Switzerland (SUPSI), Centro Galleria 2, Manno, 6928, Switzerland

[‡]Department of Mechanical, Materials and Manufacturing Engineering, University of Nottingham, NG7 2RD, United Kingdom

S Supporting Information

ABSTRACT: The construction of hierarchical materials through controlled self-assembly of molecular building blocks (e.g., dendrimers) represents a unique opportunity to generate functional nanodevices in a convenient way. Transition-metal compounds are known to be able to interact with cationic dendrimers to generate diverse supramolecular structures, such as nanofibers, with interesting collective properties. In this work, molecular dynamics simulation (MD) demonstrates that acetate ions from dissociated $\text{Cd}(\text{CH}_3\text{COO})_2$ selectively generate cationic PPI-dendrimer functional fibers through hydrophobic modification of the dendrimer's surface. The hydrophobic aggregation of dendrimers is triggered by the asymmetric nature of the acetate anions (AcO^-) rather than by the precise transition metal (Cd). The assembling directionality is also controlled by the concentration of AcO^- ions in solution. Atomic force (AFM) and transmission electron microscopy (TEM) prove these results. This well-defined directional assembly of cationic dendrimers is absent for different cadmium derivatives (i.e., CdCl_2 , CdSO_4) with symmetric anions. Moreover, since the formation of these nanofibers is controlled exclusively by selected anions, fiber disassembly can be consequently triggered via simple ionic competition by NaCl salt. Ions are here reported as a simple and cost-effective tool to drive and control actively the assembly and the disassembly of such functional nanomaterials based on dendrimers.



INTRODUCTION

The possibility to generate ordered nanostructures through controlled self-assembly is fundamental for the engineering of functional hierarchical materials with unique collective properties. Different well-defined supramolecular structures can be obtained and used for many technological applications.^{1,2} Among them, nanofibers are extremely useful to develop nanodevices with interesting optical and conductive properties for electronics,^{3,4} optics,^{5,1} sensing⁶ and biomedical applications.^{7,8} Biomolecules,⁷ and in particular dendritic molecules,⁹ can be used to generate hybrid organic–inorganic nanostructures with considerable potential for nanotechnology. Dendrimers and dendrons are hyperbranched polymers with precise symmetry and regular structures,¹⁰ which are interesting for many diverse nano- and life-science applications, for example, for gene¹¹ and drug delivery,¹² as antiviral¹³ and antibacterial agents,¹⁴ and for the construction of sensors¹⁵ and advanced materials.^{16,17} Their surface can be functionalized in a precise way to form multivalent arrays of a variety of ligands.¹⁸ The unique features of the dendritic scaffolds can give rise to many different hierarchical self-assembled structures, which are also regulated by the external conditions (pH, temperature, concentration, etc.).^{19–21} Hierarchical dendritic and polymeric aggregates can be used to direct the assembly of nanoparticles in a well-defined manner.^{22,23} For example, we have recently shown that an elastin-like polymer (ELP) is able to direct the

self-assembly of cadmium selenide (CdSe) nanoparticles prepared *in situ* to fabricate hybrid semiconductor nanofibers with interesting optical and electric properties.²⁴ The ELP polymers not only drive the formation of fibers but also stabilize and control size and spatial distribution of the CdSe nanoparticles. Recently, the possibility was reported to induce unidirectional self-assembly of fourth generation (G4) amino-terminated poly(propylene imine) (PPI) cationic dendrimers in aqueous solution containing cadmium acetate ($\text{Cd}(\text{CH}_3\text{COO})_2$) in a 10:1 salt–dendrimer molar ratio.²⁵ These PPI dendrimer-based hybrid nanofibers can be further decorated in different ways (e.g., with gold (Au) nanoparticles upon nanofiber metallization) to obtain functional hierarchical hybrid structures.

RESULTS AND DISCUSSION

Originally, the unidirectional PPI self-assembly phenomenon was associated with a hypothetical key role played by the Cd^{2+} cations.²⁵ Once added in solution, each molecule of water-soluble $\text{Cd}(\text{CH}_3\text{COO})_2$ dissociates into two negative acetate ions (CH_3COO^- or AcO^-) and a single Cd^{2+} . The initial supposition was that a single Cd^{2+} ion was able to form coordination bonds with the peripheral primary amines (NH_2)

Received: July 15, 2011

Published: January 20, 2012

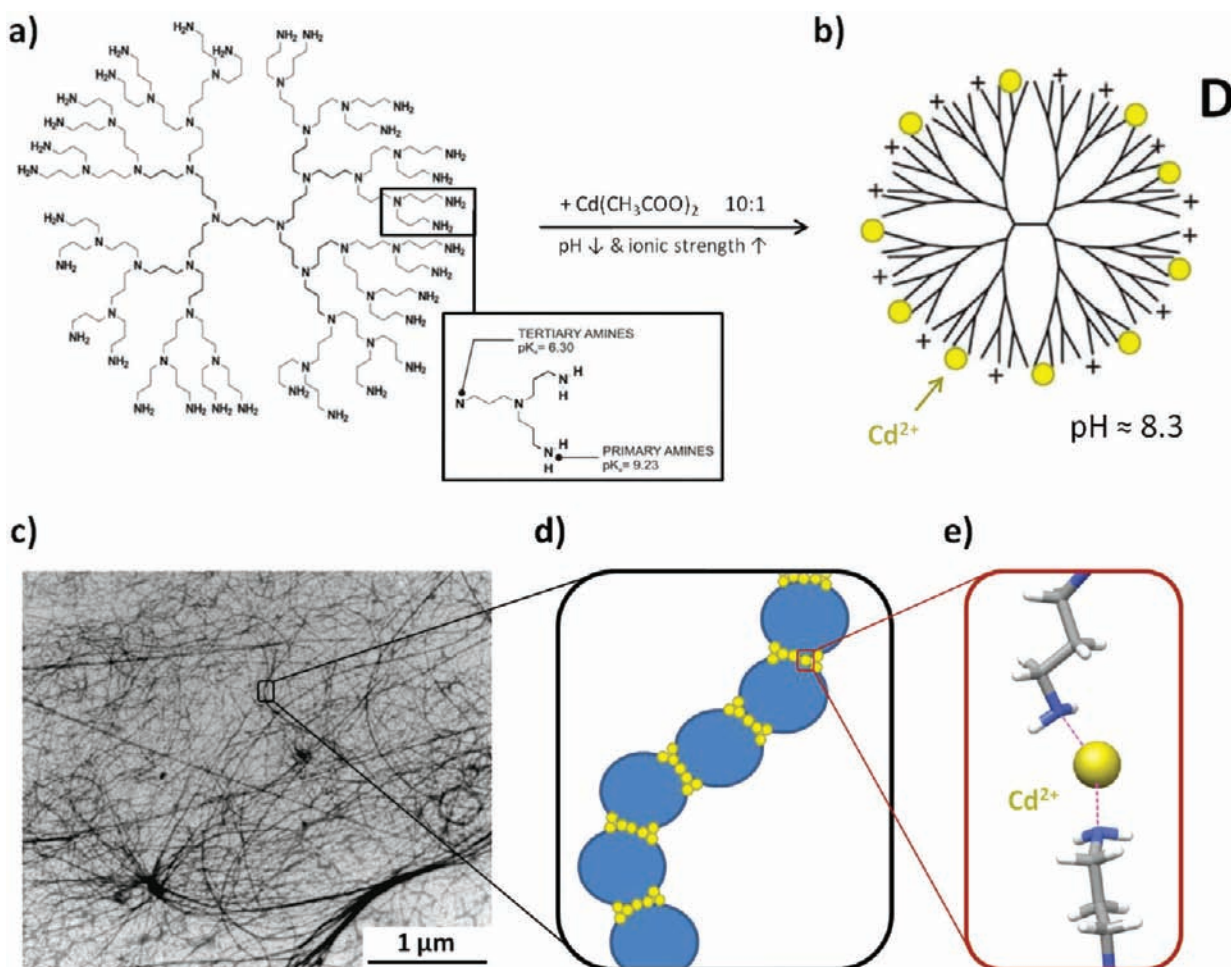


Figure 1. Original hypothesis proposed for the formation of PPI dendrimer supramolecular fibers.²⁵ (a) The addition of 3 mM of $\text{Cd}(\text{CH}_3\text{COO})_2$ in aqueous solution containing G4 PPI dendrimers (0.3 mM) decreases pH to ~ 8.3 and increases ionic strength in solution.²⁵ (b) Cd^{2+} transition metal cations coordinate to 10 PPI NH_2 surface groups, and the remaining 22 surface groups become charged (NH_3^+); each PPI dendrimer carries on average a theoretical charge of $+42e$. (c) Transmission electron microscopy (TEM) image of the fibers formed by linear complexation (d) of individual dendrimers (blue).²⁵ Cd^{2+} ions (e) were originally supposed to act as a “linker” coordinating NH_2 groups from different dendrimers leading to fiber growth.

of two different PPI dendrimers (Figure 1d) generating a web of multiple coordination “bridges” between dendrimers and leading to the formation of fibers in solution (Figure 1).²⁵ Cadmium is a transition metal, and due to its partially empty d orbital, it can generate transition complexes with those functional groups that possess lone pairs (in this case the dendrimer’s surface NH_2 groups).

The last part of this interpretation, based on the PPI linkage by Cd^{2+} ions evidenced in red in Figure 1e, presented however a few counterintuitive aspects. First, this mechanism does not explain the presence of a preferential directionality in dendrimer aggregation at any ionic concentration in solution. Second, small Cd^{2+} ions diffuse faster than bigger dendrimers in solution. Thus, it is reasonable to assume the uniform coordination of PPI dendrimers by Cd^{2+} ions as an almost immediate event as soon as $\text{Cd}(\text{CH}_3\text{COO})_2$ is dissolved in water. As a consequence, all of the dendrimers in solution can be considered as partially decorated with 10 Cd^{2+} ions and partially by protonated surface groups (22 NH_3^+) due to pH decrease induced by the increased ionic strength in solution (Figure 1b, average conditions).²⁵ This would give rise to the rapid formation of multiple positively charged dendrimers (with an average charge of $+42e$ each), which would tend to repel

each other making it impossible for dendrimer–dendrimer attraction (long-range effect) and for the consequent approaching necessary for any coordination (short-range effect). In such a case, moreover, after the sudden Cd^{2+} coordination, no free unprotonated NH_2 groups at all would be present at the dendrimer’s surface to complete the coordination as represented in Figure 1e; if the hypothesis in Figure 1b is valid for all of the dendrimers in solution, that in Figure 1e becomes unlikely.

In the present study, we used molecular dynamics (MD) simulation to explore in depth the factors that control the unidirectional dendrimer aggregation in order to have a clearer interpretation of the fiber formation phenomenon. As a first step, we created a model for generation 4 (G4) PPI dendrimer (D), whose surface groups were coordinated with 10 Cd^{2+} ions consistent with the experimental 10:1 molar ratio of cadmium acetate present in solution (Figure 1a,b and Figure S2b,c in the Supporting Information). This model aimed to represent in average the D dendrimers under experimental conditions. D was constructed and parametrized according to a well-validated procedure used by our group in previous studies on dendrimers²⁶ and dendrons²⁷ (extensive details about the computational methods and the systems simulated in this work

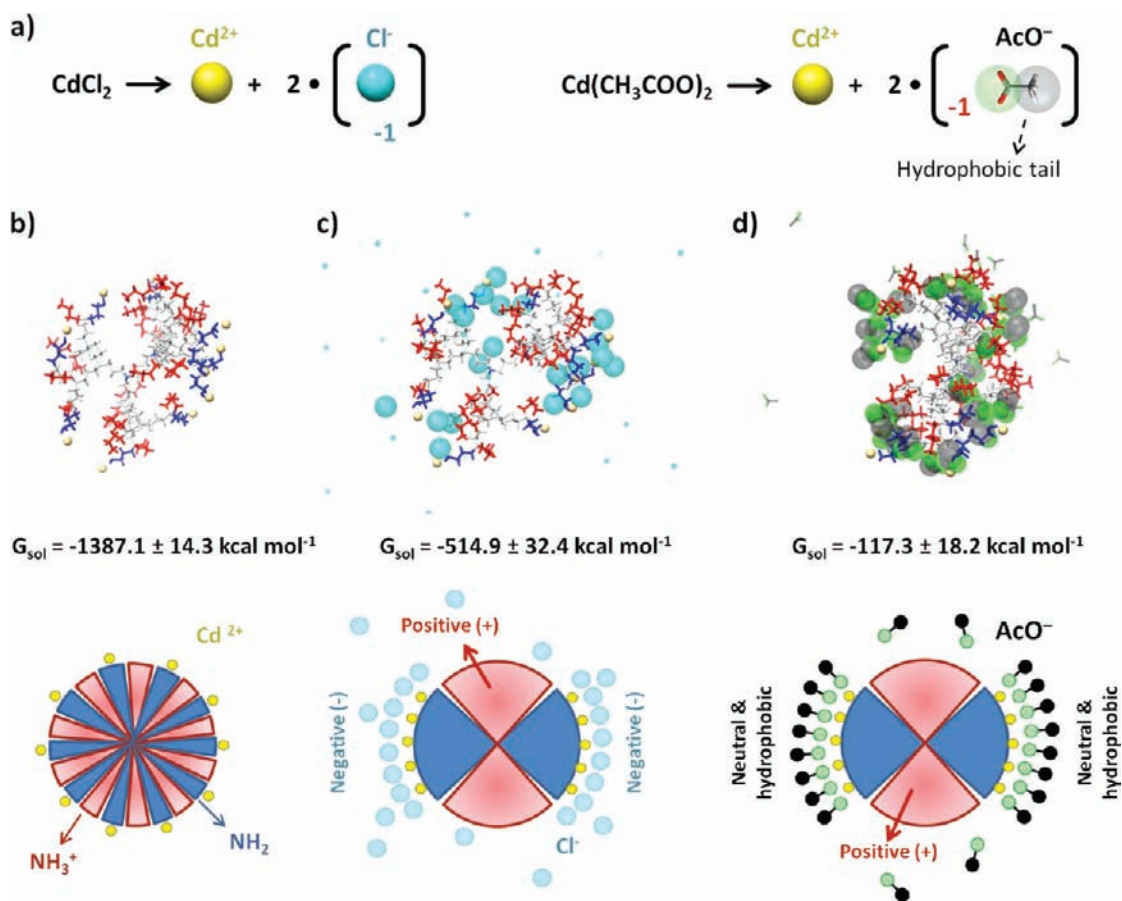


Figure 2. The effect of different ions on the dendrimer. (a) The dissociation of CdCl_2 and $\text{Cd}(\text{CH}_3\text{COO})_2$ in water introduce, respectively, Cl^- and AcO^- ions in solution. The dendrimer **D** (b) was simulated in a solution containing Cl^- (c) and AcO^- ions (d). During the MD simulations, those ions binding in a stable way to **D**'s surface are represented as spheres; those that interact only intermittently with **D** are represented as sticks. Water molecules are omitted for clarity. Cl^- (b, cyan) and AcO^- ions (c, negative heads in green and hydrophobic tails in black) accumulate and stabilize in correspondence to Cd^{2+} surface ions forming **D**– Cl^- and **D**– AcO^- dendrimer–ion primary complexes. In general, both ions modify the hydrophilicity of the dendrimer (the less negative the solvation energy, G_{sol} , the higher the hydrophobicity), but AcO^- ions render **D**– AcO^- consistently more hydrophobic than **D**– Cl^- due to the high concentration of hydrophobic CH_3 tail groups in correspondence to Cd^{2+} (d). Cl^- and AcO^- ions tend to create clusters of Cd^{2+} surface groups. The heterogeneous surface of **D**– AcO^- is consequently divided into hydrophobic neutral (NH_2 – Cd^{2+} – AcO^- in blue) and hydrophilic positive NH_3^+ domains (in red). On the other hand, when Cl^- binds to Cd^{2+} (c) the blue domains of **D**– Cl^- become negatively charged (NH_2 – Cd^{2+} – Cl^- – the negative charge present on Cl^- is directly exposed to the external solution). The schemes are illustrative, and **D**'s red and blue domains have not necessarily the same extension.

are available in the Supporting Information). The cadmium ions (10 Cd^{2+}) were coordinated uniformly and randomly to 10 of the total 32 NH_2 surface groups of the unfolded G4 PPI dendrimer. The remaining surface groups were assumed to be protonated (22 NH_3^+ groups) according to the solution pH (~ 8.3).²⁵ A single unfolded dendrimer **D** (total charge of $+42e$) was equilibrated in a periodic box containing water and AcO^- ions. All MD simulations conducted in this study were carried out in NPT conditions at 300 K and 1 atm of pressure using the AMBER 11 suite of programs²⁸ and lasted until each simulated system reached the equilibrium. The root-mean-square deviation (rmsd) data obtained from the MD trajectories were used to check the convergence to the equilibrium. The structural and energetic analyses for each system were carried out using the *ptraj* module within AMBER 11 and the MM-PBSA²⁹ approach according to a validated procedure adopted previously by our group (details about the simulations and the data analysis procedures are available in the Supporting Information).^{26,27,30,31} The same starting (unfolded) configuration of the dendrimer was also simulated as immersed in a solution of water and cadmium chloride (in the same molar

ratio of cadmium acetate, 1:10 with respect to the dendrimer). In this case, **D** was surrounded by water molecules and Cl^- ions (from dissociated CdCl_2) replacing AcO^- ones (Figure 2a). This additional system was created and simulated as a control experiment for comparison and to better interpret the coordination ability and the effect of different ions on the dendrimer assembly. Charged ions in solution are known to be capable of strong interactions with the charged surface of dendritic molecules and to interfere with the complexation between molecules.^{27,30} Most self-assembly events have hierarchical aspects and often involve different scales of supramolecular aggregation. By affecting molecular recognition, ionic strength is also known to have a direct potential impact on self-assembly.³¹

MD simulations demonstrate some interesting and important results. During the dynamics most of the Cl^- and AcO^- solution ions coordinate similarly to **D**'s surface. At **D**'s surface, the positive charge of each Cd^{2+} decorated group (NH_2 – Cd^{2+} , in blue in Figure 2) is double that present on the NH_3^+ groups (red in Figure 2) and thus the negatively charged AcO^- and Cl^- ions have consistently higher affinity for the NH_2 – Cd^{2+}

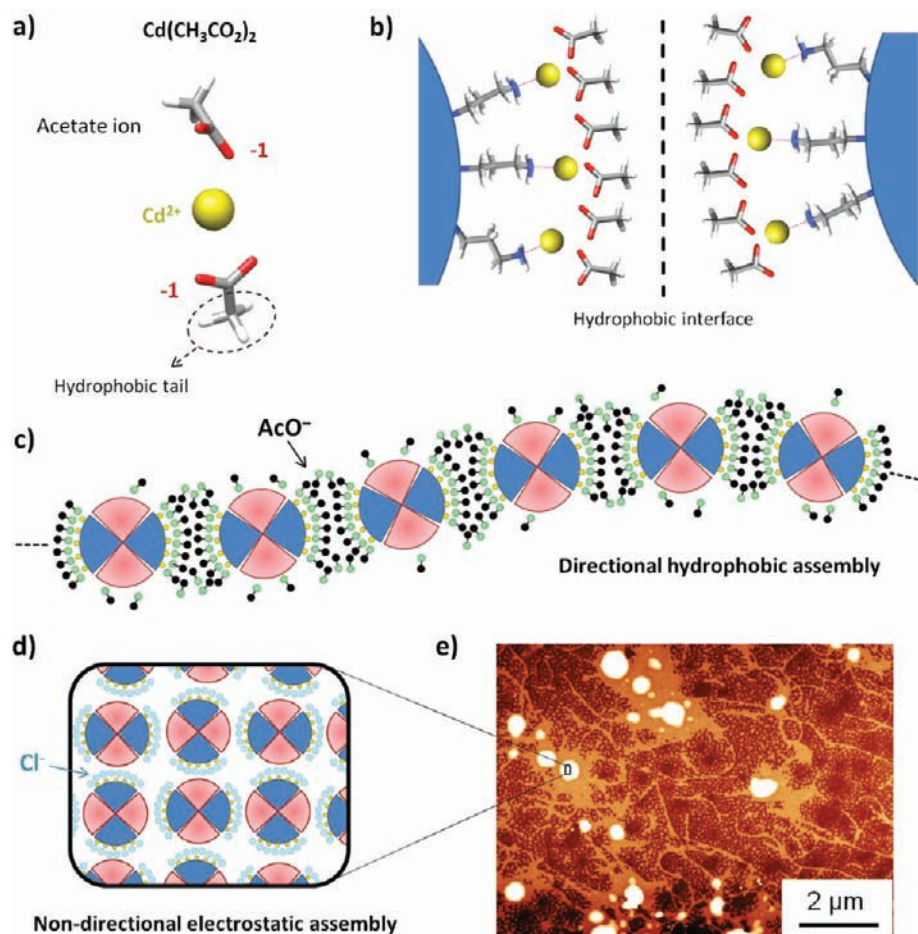


Figure 3. Ion-selective mechanism of dendrimer fibers formation. (a) The entire mechanism is controlled by acetate ions. (b) The particular features of AcO^- generate a self-assembly controlled by hydrophobic forces; the tail–tail coupling of AcO^- ions recalls the mechanism of formation of lipid bilayers and the self-assembly of amphiphiles (bolaamphiphiles).³³ (c) Dendrimer aggregation along preferential directionality is due to hydrophobic anisotropy at D 's surface, which drives aggregation of blue hydrophobic domains. (d, e) CdCl_2 (3 mM) does not generate nanofibers of PPI dendrimers (0.3 mM) in water. The nondirectional aggregation of $\text{D}-\text{Cl}^-$ complexes is generated by the electrostatic attraction between the oppositely charged red and blue surface domains, which induce the formation of multiple globular superassemblies in solution with $\sim 0.5\text{--}1\ \mu\text{m}$ size.

blue groups than for the NH_3^+ red ones. Negative ions are strongly attracted by the Cd^{2+} ions and readily coordinate to $\text{NH}_2-\text{Cd}^{2+}$ groups generating tight and stable primary dendrimer–ion complexes ($\text{D}-\text{Cl}^-$ and $\text{D}-\text{AcO}^-$ in Figure 2c,d, respectively). The affinity of Cl^- for Cd^{2+} ions is on average slightly higher than that of AcO^- ($\Delta E_{\text{attr}} = -18.1 \pm 0.8\ \text{kcal mol}^{-1}$ versus $\Delta E_{\text{attr}} = -15.6 \pm 0.8\ \text{kcal mol}^{-1}$; for AcO^- the attraction is concentrated on the negatively charged head). The dynamics of the interactions between both ions and Cd^{2+} is also rather similar (radial distribution function plots are available in the Supporting Information). The strong attraction and stable coordination between surface Cd^{2+} and the negatively charged solution ions is an intuitive phenomenon that has however an important impact particularly in the case of AcO^- . In this case, the $\text{NH}_2-\text{Cd}^{2+}$ surface groups of D are surrounded by AcO^- tails (highly hydrophobic CH_3 groups), which intuitively transform the hydrophobicity of the dendrimer (Figure 2d). Solvation energy (G_{sol}) analysis demonstrates that when AcO^- ions stabilize over D 's surface, the resulting dendrimer–ion primary complex $\text{D}-\text{AcO}^-$ is more than 10 times more hydrophobic than the native D and almost five times more hydrophobic than $\text{D}-\text{Cl}^-$ (Figure 2, less negative/favorable G_{sol}).

The electrostatic attraction between negative solution ions (Cl^- and AcO^-) and Cd^{2+} involves all of the $\text{NH}_2-\text{Cd}^{2+}$ groups, which tend to aggregate giving rise to the formation of tight surface “ionic clusters” (Figure 2b,c). In the case of AcO^- , this ionic clusterization is also more evident due to the hydrophobic association between CH_3-CH_3 AcO^- tail groups, which increase $\text{NH}_2-\text{Cd}^{2+}$ aggregation (details are available in the Supporting Information, Figure S6). As a general consequence, however, these phenomena subdivide the surface of D into “domains” where similar surface groups tend to aggregate, as represented conceptually by the schemes of Figure 2. Moreover, it is worth noting that while red domains (NH_3^+ groups) are generally hydrophilic and positively charged, the characteristics of the blue ones ($\text{NH}_2-\text{Cd}^{2+}$) depend on the coordinated anions (AcO^- or Cl^-). The presence of Cl^- , for instance, induces an overall negative charge on the D surface blue domains, while in the case of AcO^- such ions neutralize the same domains and make them strongly hydrophobic (Figure 2b,c). In this framework, NH_3^+ groups (red) interact only intermittently and discontinuously with the remaining AcO^- during the dynamics.

Within the $\text{D}-\text{AcO}^-$ primary complexes, hydrophobicity is entirely focused onto the blue domains ($\text{NH}_2-\text{Cd}^{2+}-\text{AcO}^-$ groups), which are surrounded by acetate's CH_3 tails (Figure

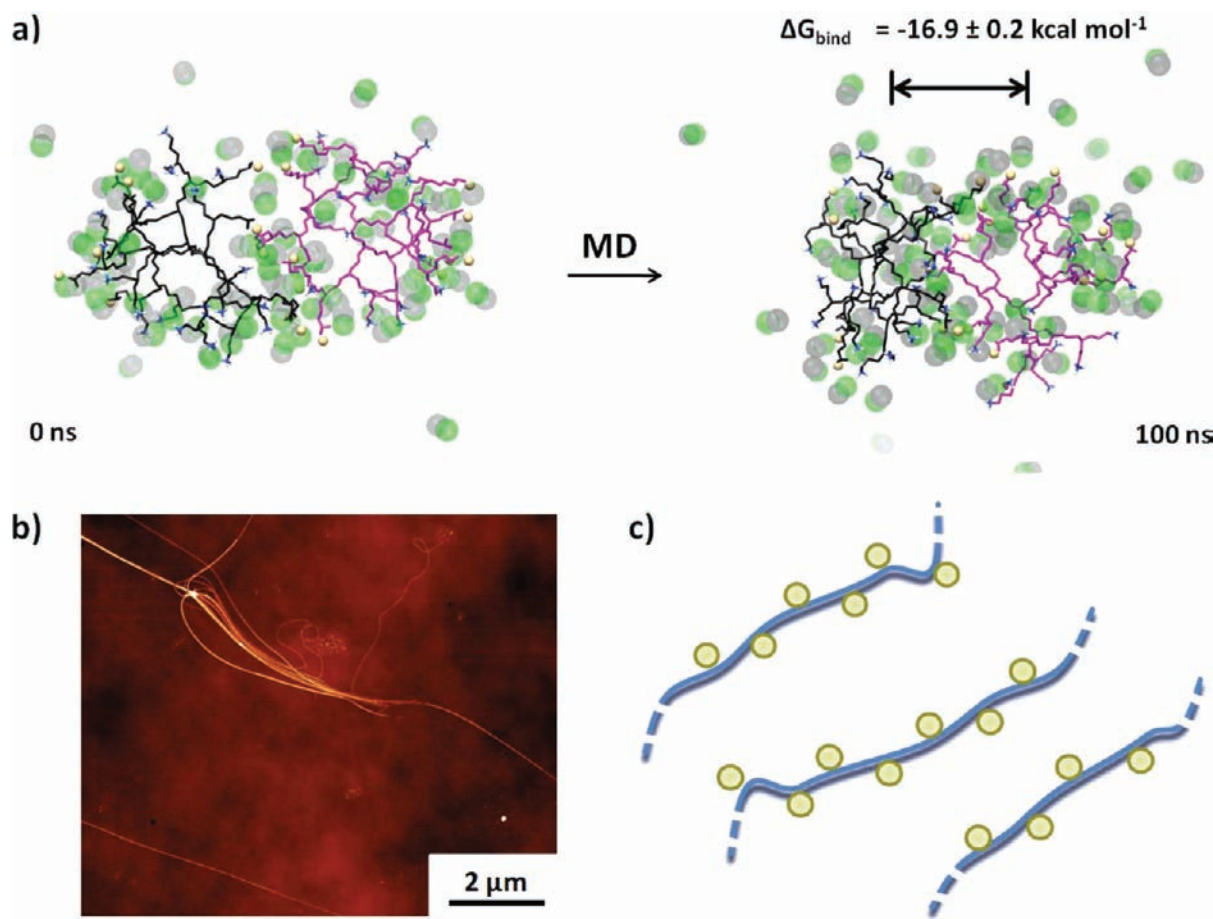


Figure 4. Snapshots taken from the MD simulation of the D1+D2–AcO⁻ secondary complex. (a) The complexation between the two D1 (black) and D2 (pink) identical dendrimers is stable over 100 ns of MD simulation (favorable ΔG_{bind}). AcO⁻ ions (green and black) act as an “ionic glue” that stabilizes the complex. The protonated amines (NH₃⁺, N and H atoms colored in blue and white, respectively) of the hydrophilic domains remain rather exposed to the solution. (b) AFM image of fiber formation on silicon substrate (which complements the TEM image of Figure 1b); PPI G4 (0.3 mM) was dissolved in a solution of distilled water and 3 mM of Cd(CH₃COO)₂. (c) Such fibers can be also functionalized, for example, with gold nanoparticles,²⁴ see also Figure S9 in the Supporting Information, or can interact with diverse precursors to achieve the *in situ* controlled formation of equidistant semiconductor domains (e.g., CdSe, see Figure S10 in the Supporting Information).

3b). The partial surface coverage of Cd²⁺ ions in concert with the ionic clustering generated by AcO⁻ transforms the symmetrical and spherical dendrimers into asymmetric building blocks (Figure 2). The hydrophobic anisotropy of D–AcO⁻ induced by ions suggests a preferential directionality for self-assembly. This result is consistent with the work conducted by Glotzer and collaborators, who identified anisotropy as a fundamental driving force to control self-assembly.³² It also proposes multiple perspectives. First, the hydrophobicity switch induced by AcO⁻ ions (Figure 3a) appears to be the main factor that triggers and controls the PPI dendrimer unidirectional assembly (Figure 3b,c). In fact, there is a clear relationship between hydrophobicity and aggregation (Figure 3b) as was also evidenced in our recent study on self-assembly of capsid viruses.³¹ Second, different from the initial hypothesis, precise ions (AcO⁻), rather than the transition metal (Cd²⁺), seem to play the major role in controlling the monodimensional dendrimer assembly in a selective way.

For instance, the different subdivision of D–Cl⁻ surface into positive NH₃⁺ (red) and negatively charged domains (blue, Figure 2c) induces a dendrimer assembly that is completely different from the one generated by AcO⁻, a nondirectional aggregation resulting from the electrostatic attraction between the oppositely charged red (NH₃⁺) and blue (NH₂–Cd²⁺–Cl⁻)

domains of different D–Cl⁻ primary complexes (Figure 3d). AFM investigations show that in a solution containing 3 mM CdCl₂, no formation of fibers occurs for the same dendrimers (PPI concentration of 0.3 mM) under the same conditions, demonstrating the absence of any assembly directionality. In this case, spherical aggregates with diameter of about ~0.5–1 μm are formed as shown in Figure 3e. This lack of directionality in the assembly was also verified for different transition-metal based salts (see, for instance, Figure S11 and related comments in the Supporting Information). As a third point, the peculiar partition of D’s surface into different red and blue surface domains (Figure 3) is intrinsically dependent upon the ionic concentration in solution owing to the partial Cd²⁺ coordination of the dendrimer surface (in this case, only 10 NH₂ groups coordinate to Cd²⁺). This evidence implies the existence of a precise “window” of dendrimer–salt molar ratios allowing for such directionality. This was proven by further control experiments; AFM measurements demonstrated that already at 1:20 dendrimer–Cd(CH₃COO)₂ molar ratio, the assembly loses directionality and the fibers are almost entirely replaced by supramolecular assemblies with globular shape (see Supporting Information, Figure S8). This strong evidence confirms that the nature of ions and their concentration in solution control actively the assembling of dendrimers and the

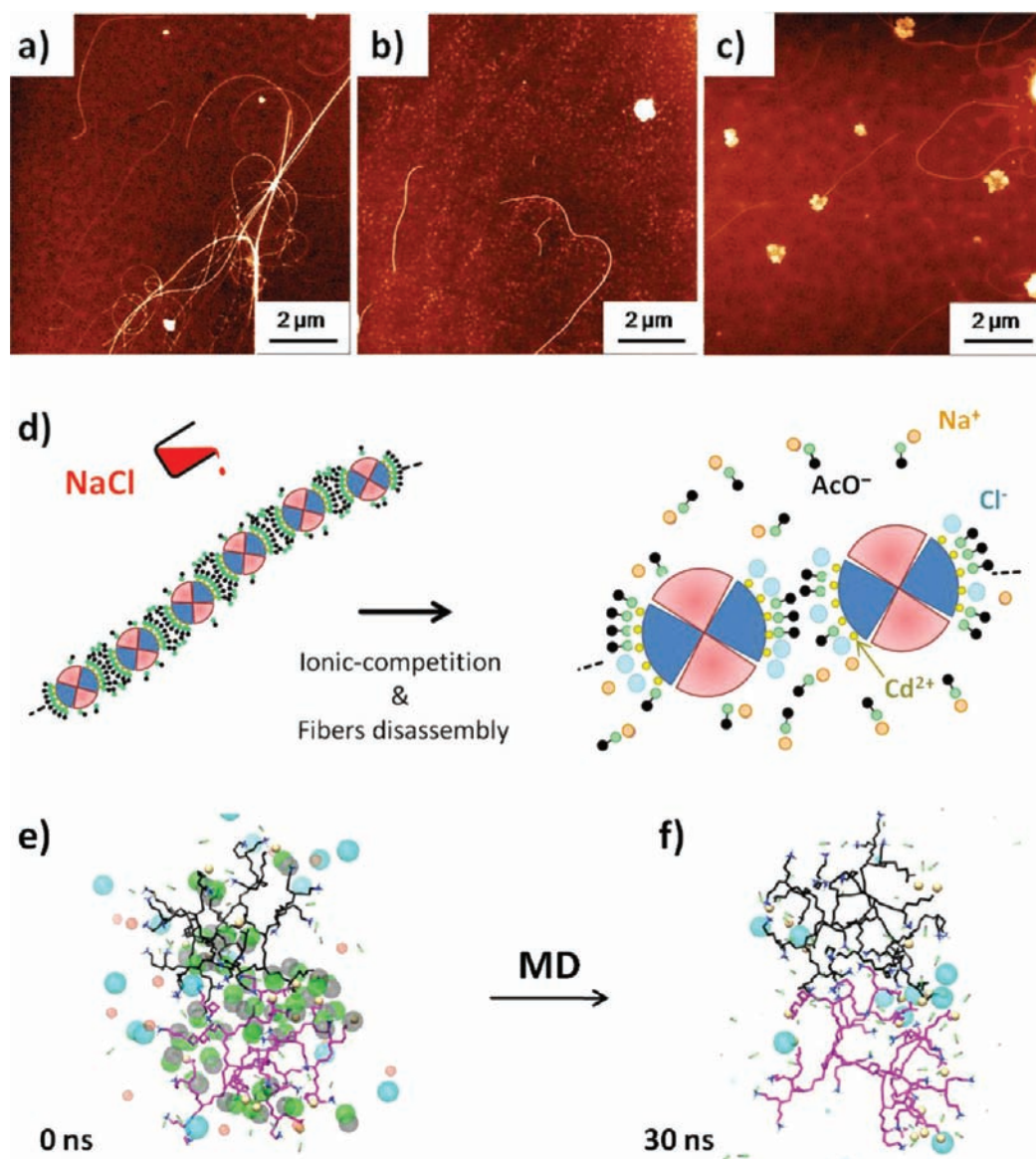


Figure 5. Fiber disassembly triggered by ionic competition. (a) AFM image of PPI- $\text{Cd}(\text{CH}_3\text{COO})_2$ nanofibers on silicon substrate. Fibers are formed upon dissolving 0.3 mM PPI G4 dendrimer in distilled water solution with 3 mM $\text{Cd}(\text{CH}_3\text{COO})_2$ (a molecular ratio with the dendrimers of 10:1). (b) After the addition of only 0.3 mM NaCl in solution (1:1 molar ratio with the dendrimer) most of the dendrimer fibers start to disassemble and to disappear from the solution substituted by a general dispersity. (c) When the NaCl salt concentration is increased to 3 mM (the same concentration in solution of cadmium acetate), the fibers start to be replaced by particles as was evidenced in CdCl_2 solution (Figure 3e). (d) Fiber disassembly is induced by ionic competition; at D's surface Cl^- ions (cyan) replace AcO^- ions (green and black) due to a higher affinity for Cd^{2+} (yellow). (e) The 100 ns MD simulation of Figure 4a was continued with the addition of 20 NaCl molecules to the solution (10:1 molecular ratio with the dendrimers). Cl^- starts to replace AcO^- in correspondence of Cd^{2+} ions after only 30 ns. Within the snapshots D1 and D2 are colored in black and pink. Cl^- and Na^+ are colored in cyan and orange; water is not shown for clarity. (f) After 30 ns, only those Cl^- that replace AcO^- and coordinate stably with the dendrimers (Cd^{2+}) are represented as cyan spheres.

aggregation directionality as represented in Figure 3. Similar results were reported in recent work by the groups of Geng and Newkome who demonstrated that the electrostatic interactions between spherical dendrimers and symmetric ions can result in the formation of capsules³⁴ or supramolecular fibers.³⁵ Precise stoichiometries between dendrimer surface NH_2 groups and Cd^{2+} and AcO^- ions could suggest a general pattern in self-assembly of dendrimer-based fibers in the framework of what was recently proposed by Tomalia.³⁶ However, this would need deeper investigation to be considered a general concept due to the potential key role played by many dendritic structural

parameters (e.g., rigidity/flexibility of the scaffold, dendritic generation, etc.).

As a next step, a new molecular system to represent the interface between two D dendrimers inside the fiber (Figure 3b,c) was created. The equilibrated configuration of the D- AcO^- primary complex (Figure 2d) was taken as a reference. D- AcO^- was duplicated, and two identical D1- AcO^- and D2- AcO^- primary complexes were put in close contact (Figure 4a); the surface regions with the highest concentration of Cd^{2+} (and AcO^-) were coupled to form the interface. The consequent secondary D1+D2- AcO^- complex was again solvated and simulated for 100 ns to prove the stability of

the complexation. The hypothesis presented in Figure 3 finds consistency and confirmation in this simulation. The **D1+D2**– AcO^- secondary complex remains, in fact, stable over the entire 100 ns MD run (Figure 4a). During the dynamics, AcO^- ions act as a real “ionic glue” that solidifies (clusters) at the interface between the two dendrimers stabilizing the complex (a movie of this simulation is provided in the Supporting Information). The free energy of binding between the two primary complexes (**D1**– AcO^- and **D2**– AcO^-) was also obtained from the equilibrated phase MD trajectories (Figure 4a, ΔG_{bind} ; complete energy data are reported in the Supporting Information).

The favorable value of ΔG_{bind} demonstrates that AcO^- ions stabilize the aggregation between **D1** and **D2** dendrimers leading to stable complexation ($\Delta G_{\text{bind}} = -16.9 \pm 0.2 \text{ kcal mol}^{-1}$). AcO^- ions screen the positive charges present on the surfaces of the **D1** and **D2** dendrimers (+42e each), which otherwise would give rise to strong electrostatic repulsion. At the same time, they enhance the hydrophobicity of the two dendrimers, which aggregate to minimize the hydrophobic surface exposed to the polar solvent (hydrophobic assembly). Together, this simulation and the conceptual scheme of Figure 3c identify also the positively charged domains (NH_3^+) and the hydrophobic and neutral **D1**–**D2**– AcO^- interface zones as the potential binding sites along the fiber for eventual functionalization with negatively charged or neutral nanoparticles, respectively (e.g., gold, CdSe, etc.). The fact that this monodimensional aggregation of dendrimers into nanofibers is controlled only by the particular nature and by the number of AcO^- ions present in solution makes of this assembly phenomenon a real “ion-selective” process.

Since the mechanism is entirely governed by ions, these results suggested that it was also intuitively possible to use other ions to trigger disassembly. Our intuition proposed that to disassemble such functional fibers (Figure 5a) it was in principle sufficient to introduce in the system competitive negative ions with higher Cd^{2+} affinity than that of AcO^- that do not alter the hydrophobicity of the dendrimers (e.g., Cl^-). As an easy and cheap example, we tested NaCl salt, which is highly soluble in water and introduces Cl^- ions as competitors for the AcO^- in solution. Figure 5 demonstrates the efficacy of this principle.

As soon as 0.3 mM NaCl is introduced into the hybrid system (Figure 5a), the nanofibers start to disassemble rapidly (Figure 5b). Moreover, when the NaCl concentration is increased to 3 mM (Figure 5c), the fibers start to be substituted by globular aggregates with ~ 0.5 – $1 \mu\text{m}$ size, very similar to those generated by dendrimers in CdCl_2 solution (Figure 3e). This disassembly process is due to ion competition; Cl^- ions replace AcO^- ions at the dendrimer's surface, and AcO^- ions diffuse in solution (Figure 5d). It is evident that the presence of Cl^- at **D**'s surface eliminates the hydrophobic surface anisotropy, which controls the unidirectional assembly. The presence of ionic competition and substitution is also proven by modeling. The 100 ns **D1**–**D2**– AcO^- MD simulation (Figure 4a) was continued after the addition of 20 NaCl molecules in solution (1:1 molar ratio with $\text{Cd}(\text{CH}_3\text{COO})_2$). Figure 5f demonstrates that the higher affinity of Cl^- for Cd^{2+} provokes consistent ionic substitution in correspondence with Cd^{2+} ions and at the interface between the two dendrimers after only 30 ns of simulation (9 Cl^- of the total 20 are already coordinated tightly to Cd^{2+} replacing AcO^- ions).

CONCLUSIONS

In conclusion, we have reported a simple concept to control the assembly of functional nanofibers based on amino-terminated dendrimers (PPI) using selectively determined ions in an active way. Such fibers have already been demonstrated to possess interesting functionalities and properties; in fact they can be functionalized in different ways to obtain hybrid conductor or semiconductor nanodevices.²⁵ The monodimensional aggregation of multiple dendrimers and the consequent fiber growth in a solution of cadmium acetate is demonstrated to be due to the AcO^- ions rather than to the particular transition metal (Cd^{2+}). AcO^- ions in fact can direct the assembly of dendrimers through surface hydrophobic modification. The aggregation directionality is also controlled actively by the ionic concentration, which subdivides the dendrimer's surface into hydrophobic and hydrophilic domains leading to preferential directions of aggregation. Self-assembly and aggregation directionality are both governed exclusively by ions, making this nanofiber formation mechanism a real “ion-selective” process. As a consequence, we have also demonstrated that fiber disassembly can be easily triggered via ionic competition by using simple NaCl salt.

This study reports a general principle according to which it is possible to use determined ions to trigger and control the directional assembly of a variety of dendritic structures of which the surface is decorated by amino groups possessing lone pairs (NH_2 ; in practice, the majority of the most common cationic dendrimers). These results can have a consistent impact on different fields of nanotechnology, opening new routes for the development of a novel family of facile and more “sustainable” functional materials for technological applications. In fact, since the particular transition metal (Cd^{2+}) is demonstrated not to play a major role in the fiber formation process, the cadmium-based precursor could be in principle replaced; future efforts will be addressed to test different cadmium-free derivatives with similar characteristics (e.g., $\text{Fe}(\text{CH}_3\text{COO})_2$, etc.). At the same time, the possibility to disassemble such functional fibers through simple and easy ionic competition using cheap NaCl salt suggests intriguing perspectives for the development of new technological nanomaterials with low environmental impact.

ASSOCIATED CONTENT

Supporting Information

Detailed information about the computational methods, the creation and parametrization of the molecular systems simulated in this work, energetic and structural analysis and structural data (RDF plots, averaged distances, etc.), additional AFM and TEM images, and a movie (AVI format) of the MD simulation of the dendrimer aggregation. This material is available free of charge via the Internet at <http://pubs.acs.org>.

AUTHOR INFORMATION

Corresponding Author

amir.fahmi@hrw.de; giovanni.pavan@supsi.ch

Present Address

[§]Faculty Technology and Bionics, Rhein-Waal University of Applied Sciences, D-46446 Emmerich, Germany

Notes

The authors declare no competing financial interest.

■ ACKNOWLEDGMENTS

The authors acknowledge the COST action TD0802, 'Dendrimers in Biomedical Applications', in favoring this collaborative research program. Dr. Marek Maly is thankfully acknowledged for useful discussions. M.G., A.D., and G.M.P. were supported by DECS-Canton Ticino and by SER-COST. N.C. and A.F. acknowledge the funding from the UK Engineering and Physical Sciences Research Council (EPSRC) through the Nottingham Innovative Manufacturing Research Centre (NIMRC).

■ REFERENCES

(1) (a) Huynh, W. U.; Dittmer, J. J.; Alivisatos, P. A. *Science* **2002**, *295*, 2425–2427. (b) Yu, G.; Lieber, C. M. *Pure Appl. Chem.* **2010**, *82*, 2295–2314.

(2) (a) Alivisatos, A. P. *Science* **1996**, *271*, 933–937. (b) Empedocles, S. A.; Bawendi, M. G. *Science* **1997**, *278*, 2114.

(3) (a) Duan, X. F.; Huang, Y.; Cui, Y.; Wang, J. F.; Lieber, C. M. *Nature* **2001**, *409*, 66. (b) Gudiksen, M. S.; Lauhon, L. J.; Wang, J.; Smith, D. C.; Lieber, C. M. *Nature* **2002**, *415*, 617.

(4) Fuhrer, M. S.; Nygard, J.; Shih, L.; Forero, M.; Yoon, Y. G.; Mazzone, M. S. C.; Choi, H. J.; Ihm, J.; Louie, S. G.; Zettl, A.; McEuen, P. L. *Science* **2000**, *288*, 494.

(5) Klimov, V. I.; Mikhailovsky, A. A.; Xu, S.; Malko, A.; Hollingsworth, J. A.; Leatherdale, C. A.; Eisler, H. J.; Bawendi, M. G. *Science* **2000**, *290*, 314.

(6) Kong, J.; Franklin, N. R.; Zhou, C. W.; Chapline, M. G.; Peng, S.; Cho, K. J.; Dai, H. J. *Science* **2000**, *287*, 622.

(7) Bruchez, M.; Moronne, M.; Gin, P.; Weiss, S.; Alivisatos, A. P. *Science* **1998**, *281*, 2013.

(8) (a) Chan, W. C. W.; Nie, S. M. *Science* **1998**, *281*, 2016. (b) Taton, T. A.; Mirkin, C. A.; Letsinger, R. L. *Science* **2000**, *289*, 1757.

(9) (a) Wang, Q.; Mynar, J. L.; Yoashida, M.; Lee, E.; Lee, M.; Okuro, K.; Kinbara, K.; Aida, T. *Nature* **2010**, *463*, 339–343. (b) Okuro, K.; Kinbara, K.; Takeda, K.; Inoue, Y.; Ishijima, A.; Aida, T. *Angew. Chem., Int. Ed.* **2010**, *49*, 3030–3033. (c) Toma, F. M.; Sartorel, A.; Iurlo, M.; Carraro, M.; Parisse, P.; Maccato, C.; Rapino, S.; Gonzalez, B. R.; Amenitsch, H.; Da Ros, T.; Casalis, L.; Goldoni, A.; Marcaccio, M.; Scorrano, G.; Scoles, G.; Paolucci, F.; Prato, M.; Bonchio, M. *Nat. Chem.* **2010**, *10*, 826–831.

(10) Astruc, D.; Boisselier, E.; Ornelas, C. *Chem. Rev.* **2010**, *110*, 1857–1959.

(11) (a) Ferber, D. *Science* **2001**, *294*, 1638–1642. (b) Guillot-Nieckowski, M.; Eisler, S.; Diederich, F. *New J. Chem.* **2007**, *31*, 1111–1127. (c) Kukowska-Latallo, J. F.; Bielinska, A. U.; Johnson, J.; Spindler, R.; Tomalia, D. A.; Baker, J. R. *Proc. Natl. Acad. Sci. U.S.A.* **1996**, *93*, 4897–4902.

(12) Amir, R. J.; Albertazzi, L.; Willis, J.; Khan, A.; Kang, T.; Hawker, C. J. *Angew. Chem., Int. Ed.* **2011**, *50*, 3425–3429.

(13) Rupp, R.; Rosenthal, S. L.; Stanberry, L. R. *Int. J. Nanomed.* **2007**, *2*, 561–566.

(14) Roy, R. *Curr. Opin. Struct. Biol.* **1996**, *6*, 692–702.

(15) Albertazzi, L.; Storti, B.; Marchetti, L.; Beltram, F. *J. Am. Chem. Soc.* **2010**, *132*, 18158–18167.

(16) (a) Tong, G. J.; Hsiao, S. C.; Carrico, Z. M.; Francis, M. B. *J. Am. Chem. Soc.* **2009**, *131*, 11174–11178. (b) Wesley, W.; Hsiao, S. C.; Carrico, Z. M.; Francis, M. B. *Angew. Chem., Int. Ed.* **2009**, *48*, 9493–9497. (c) Yoo, P. J.; Nam, K. T.; Qi, J.; Lee, S.-K.; Park, J.; Belcher, A. M.; Hammond, P. T. *Nat. Mater.* **2006**, *5*, 234–240.

(17) (a) Ercolani, G. *J. Am. Chem. Soc.* **2003**, *125*, 16097–16103. (b) Mann, S. *Nat. Mater.* **2009**, *8*, 781–792. (c) Whitesides, G. M.; Grzybowski, B. *Science* **2002**, *295*, 2418–2421. (d) Okuro, K.; Kinbara, K.; Tsumoto, K.; Ishii, N.; Aida, T. *J. Am. Chem. Soc.* **2009**, *131*, 1626–1627. (e) Herrero, M. A.; Toma, F. M.; Al-Jamal, K. T.; Kostarelos, K.; Bianco, A.; Da Ros, T.; Bano, F.; Casalis, L.; Scoles, G.; Prato, M. *J. Am. Chem. Soc.* **2009**, *131*, 9843–9848.

(18) (a) Newkome, G. R.; Shreiner, C. *Chem. Rev.* **2010**, *110*, 6338–6442. (b) Fréchet, J. M. J. *Proc. Natl. Acad. Sci. U.S.A.* **2002**, *99*, 4782–4787.

(19) (a) Fahmi, A.; D'Aleo, A.; Williams, R. M.; De Cola, L.; Gindy, N.; Vögtle, F. *Langmuir* **2007**, *23*, 7831–7835. (b) Fahmi, A.; Barragan, S. P.; D'Aleo, A.; Williams, R. M.; van Heyst, J.; De Cola, L.; Vögtle, F. *Mater. Chem. Phys.* **2007**, *103*, 361–365. (c) Percec, V.; Wilson, D. A.; Leowanawat, P.; Wilson, C. J.; Hughes, A. D.; Kaucher, M. S.; Hammer, D. A.; Levine, D. H.; Kim, A. J.; Bates, F. S.; Zhang, K. P.; Lodge, T. P.; Klein, M. L.; DeVane, R. H.; Aqad, E.; Rosen, B. M.; Argintau, A. O.; Sienkowska, M. J.; Rissanen, K.; Nummelin, S.; Ropponen, J. *Science* **2010**, *328*, 1009–1014.

(20) (a) Heyen, A.; Buron, C. C.; Tianshi, Q.; Bauer, R.; Jonas, A. M.; Müllen, K.; De Schryver, F. C.; De Feyter, S. *Small* **2008**, *4*, 1160–116. (b) Qi, X.; Xue, C.; Huang, X.; Huang, Y.; Zhou, X.; Li, H.; Liu, D.; Boey, F.; Yan, Q.; Huang, W.; De Feyter, S.; Müllen, K.; Zhang, H. *Adv. Funct. Mater.* **2010**, *20*, 43–49. (c) Kim, H. J.; Kim, T.; Lee, M. *Acc. Chem. Res.* **2011**, *44*, 72–82.

(21) (a) Franc, G.; Badetti, E.; Colliere, V.; Majoral, J.-P.; Sebastian, R. M.; Caminade, A.-M. *Nanoscale* **2009**, *1*, 233–237. (b) Hermans, T. M.; Broeren, M. A. C.; Gomopoulos, N.; van der Schoot, P.; van Genderen, M. H. P.; Sommerdijk, N. A. J. M.; Fytas, G.; Meijer, E. W. *Nat. Nanotechnol.* **2009**, *4*, 721–726. (c) Lee, M.; Im, J.; Lee, B. Y.; Myung, S.; Kang, J.; Huang, L.; Kwon, Y. K.; Hong, S. *Nat. Nanotech.* **2006**, *1*, 66–71.

(22) De, M.; Ghosh, P. S.; Rotello, V. M. *Adv. Mater.* **2008**, *20*, 4225–4241.

(23) (a) Kogan, M. J.; Olmedo, I.; Hosta, L.; Guerrero, A. R.; Cruz, L. J.; Albericio, F. *Nanomedicine* **2007**, *2*, 287. (b) Tkachenko, A. G.; Xie, H.; Coleman, D.; Glomm, W.; Ryan, J.; Anderson, M. F.; Franzen, S.; Feldheim, D. L. *J. Am. Chem. Soc.* **2003**, *125*, 4700.

(24) Fahmi, A.; Pietsch, T.; Bryszewska, M.; Rodriguez-Cabello, J. C.; Koceva-Chyla, A.; Arias, F. J.; Rodrigo, M. A.; Gindy, N. *Adv. Funct. Mater.* **2010**, *20*, 1011–1018.

(25) Pietsch, T.; Cheval, N.; Appelhans, D.; Gindy, N.; Voit, B.; Fahmi, A. *Small* **2011**, *7*, 221–225.

(26) (a) Pavan, G. M.; Albertazzi, L.; Danani, A. *J. Phys. Chem. B* **2010**, *114*, 2667–2675. (b) Jensen, L. B.; Mortensen, K.; Pavan, G. M.; Kasimova, M. R.; Jensen, D. K.; Gadzhayeva, V.; Nielsen, H. M.; Foged, C. *Biomacromolecules* **2010**, *11*, 3571–3577.

(27) (a) Pavan, G. M.; Kostianen, M. A.; Danani, A. *J. Phys. Chem. B* **2010**, *114*, 5686–5693. (b) Pavan, G. M.; Danani, A.; Priol, S.; Smith, D. K. *J. Am. Chem. Soc.* **2009**, *131*, 9686–9694.

(28) Case, D. A.; Darden, T. A.; Cheatham, T. E., III; Simmerling, C. L.; Wang, J.; Duke, R. E.; Luo, R.; Walker, R. C.; Zhang, W.; Merz, K. M.; Robertson, B.; Wang, B.; Hayik, S.; Roitberg, A.; Seabra, G.; Kolossvary, I.; Wong, K. F.; Paesani, F.; Vanicek, J.; Liu, J.; Wu, X.; Brozell, S.; Steinbrecher, T.; Gohlke, H.; Cai, Q.; Ye, X.; Wang, J.; Hsieh, M.-J.; Cui, G.; Roe, D. R.; Mathews, D. H.; Seetin, M. G.; Sangui, C.; Babin, V.; Luchko, T.; Gusarov, S.; Kovalenko, A.; Kollman, P. A. *AMBER 11*; University of California: San Francisco, CA, 2010.

(29) Srinivasan, J.; Cheatham, T. E.; Cieplak, P.; Kollman, P. A.; Case, D. A. *J. Am. Chem. Soc.* **1998**, *120*, 9401–9409.

(30) (a) Pavan, G. M.; Danani, A. *Phys. Chem. Chem. Phys.* **2010**, *12*, 13914–13917. (b) Kostianen, M. A.; Kotimaa, J.; Laukkanen, M. L.; Pavan, G. M. *Chem.—Eur. J.* **2010**, *16*, 6912–6918.

(31) Doni, G.; Kostianen, M. A.; Danani, A.; Pavan, G. M. *Nano Lett.* **2011**, *11*, 723–728.

(32) (a) Glotzer, S. C.; Solomon, M. J. *Nat. Mater.* **2007**, *6*, 557–562. (b) Glotzer, S. C. *Science* **2004**, *306*, 419–420.

(33) Escamilla, G. H.; Newkome, G. R. *Angew. Chem., Int. Ed.* **1994**, *33*, 1937–1940.

(34) Ju, R.; Tessier, M.; Olliff, L.; Woods, R.; Summers, A.; Geng, Y. *Chem. Commun.* **2011**, *47*, 268–270.

(35) Wang, P.; Moorefield, C. N.; Jeong, K. U.; Hwang, S.-H.; Sinan, L.; Cheng, S. Z. D.; Newkome, G. R. *Adv. Mater.* **2008**, *20*, 1381–1385.

(36) (a) Tomalia, D. A. *Soft Matter* **2010**, *6*, 456–474. (b) Tomalia, D. A. *J. Nanopart. Res.* **2009**, *11*, 1251–1310.